

Low Temperature Synthesis of Transparent, Vertically Aligned Anatase TiO₂ Nanowire Arrays: Application to Dye Sensitized Solar Cells

Su-II In, Klaus P. Almtoft,[†] Hyeonseok Lee, Inge H. Andersen,[†] Dongdong Qin, Ningzhong Bao,[‡] and C. A. Grimes^{§,*}

Department of Chemistry and Department of Electrical Engineering, the Pennsylvania State University,
State College, PA 16802, USA

[†]Danish Technological Institute, Tribology Centre, Kongsvang Allé 29, DK-8000 Aarhus C, Denmark

[‡]State Key Laboratory of Materials-Oriented Chemical Engineering, Nanjing University of Technology, Nanjing,
Jiangsu 210009, China

[§]Flux Photon Corporation, 620 Hutton Street, Raleigh, NC 27606, USA. *E-mail: craig.grimes40@gmail.com

Received December 14, 2011, Accepted March 19, 2012

We present a low temperature (≈ 70 °C) method to prepare anatase, vertically aligned feather-like TiO₂ (VAFT) nanowire arrays *via* reactive pulsed DC magnetron sputtering. The synthesis method is general, offering a promising strategy for preparing crystalline nanowire metal oxide films for applications including gas sensing, photocatalysis, and 3rd generation photovoltaics. As an example application, anatase nanowire films are grown on fluorine doped tin oxide coated glass substrates and used as the photoanode in dye sensitized solar cells (DSSCs). AM1.5G power conversion efficiencies for the solar cells made of 1 μ m thick VAFT have reached 0.42%, which compares favorably to solar cells made of the same thickness P25 TiO₂ (0.35%).

Key Words : Anatase, Titanium dioxide, Nanowire, Nanowire array

Introduction

Since the initial work of O’regan and Grätzel,¹ considerable effort has been focused on the development of dye-sensitized solar cells (DSSCs) with anatase TiO₂ as the ‘gold standard’ photoanode material.² Anatase photoanodes offer a stable chemical interface for dye absorption, and also a photoanode comprised of nanoparticles offers high surface area which enhances light absorption. However, a fundamental drawback of the nanoparticle film structure is that the photogenerated electron must travel from nanoparticle-to-nanoparticle to reach the back contact. The random nanoparticle-to-nanoparticle pathway offers the opportunity for unwanted charge recombination. Improving rates of electron transport and interfacial electron transfer within the photoanodes would enable the use of thicker layers for greater light absorption without a penalty of increased charge recombination.³ One approach to achieve higher DSSC photoconversion efficiencies is through the use of high surface area, vertically oriented, one dimensional (1-D) TiO₂ nanotube/nanowire array films.³⁻⁷ Films comprised of self-organized TiO₂ nanowire/nanotube arrays vertically oriented from a transparent conducting oxide (TCO) substrate offer (1) large surface areas for dye sensitization, which results in enhanced light harvesting; (2) easy transfer of electrons injected from the photo-excited dye; (3) vectorial (directed) charge transport to the electrical contact; and (4) a readily accessible space for intercalation of the redox electrolyte or p-type semiconductor. However, while self-assembled and vertically oriented 1-D titania nano-architected films offer great potential for enhancing the efficiency of 3rd generation photovoltaics to date, such a

breakthrough has yet to be achieved due to limitations inherent in the 1-D titania architectures. For example, anatase TiO₂ nanotube arrays on fluorine doped tin oxide (FTO) coated glass of desired pore size and length can be achieved by anodic oxidation^{8,9} followed by an annealing step to induce crystallization. The length and pore size of the nanotube arrays can be easily controlled by (1) choosing a suitable anodization electrolyte composed of an organic solvent with appropriate concentration of fluoride ions; and (2) utilizing conductivity modifying additives- if so desired; as well as (3) changing the anodization voltage range.¹⁰⁻¹⁴ While fabrication of nanotube arrays on FTO coated glass is not simplistic, polycrystalline anatase TiO₂ nanotube arrays up to 53 μ m in length have been achieved on FTO-coated glass.⁵ However the elevated temperature annealing step required to crystallize the amorphous as-anodized nanotubes degrades the conductivity of the underlying FTO layer, therefore increasing the series resistance.¹⁵ Another approach to achieving self-assembled and vertically oriented single crystal 1-D TiO₂ nanostructured films, (in this case rutile nanowires), is by hydrothermal synthesis.^{6,7} Yet, in comparison to anatase, the lower conduction band level of rutile results in a lower open circuit voltage. Furthermore, for equal degrees of crystallization, the charge transport properties of rutile are inferior to those of anatase.

Hope remains, at least in the opinion of the authors, that self-assembled 1-D nanostructured anatase films may yet revolutionize 3rd generation photovoltaics. In this work, we present a new sputter-deposition approach for achieving polycrystalline anatase phase and vertically aligned feather-like TiO₂ nanowire arrays on fluorine doped tin oxide coated glass substrates, obtained *via* a one step deposition technique

performed at low temperature ($\sim 70^\circ\text{C}$) with the conductivity of the FTO coated glass substrate unaffected.

Experimental

Nanowire Synthesis. Anatase nanowire arrays were grown on FTO coated glass (TEC-8, $8\ \Omega$ per square) by reactive, pulsed DC magnetron sputtering using an industrial Ceme-Con CC800/9 SinOx coating unit with a $850 \times 850 \times 1000\ \text{mm}^3$ chamber size. The sputtering chamber was equipped with four magnetrons-each mounted with a $500 \times 88\ \text{mm}$ Ti target (purity 99.5 wt %). A pulsed DC power of 500 W was applied to each magnetron. Depositions were carried out in an Ar/O₂ atmosphere, where the oxygen acted as the reactive gas for the nanowire array formation at a total pressure of about 400 mPa. The Ar-O₂ gas flow ratio was 350 sccm-60 sccm, resulting in stoichiometric films. The substrates were mounted on a rotating sample stage carrying out a 2-fold planetary rotation in order to achieve a uniform coating. Prior to film deposition, the chamber was pumped to a pressure of 4 mPa and subsequently the electrically floating substrates were pre-heated to a deposition temperature of $\approx 423\ \text{K}$ by use of a resistive heater. The deposition rate was approximately $1\ \text{nm min}^{-1}$.

Solar Cell Fabrication. Nanowire array samples were coated with dye through immersion overnight in a 0.3 mM solution (ethanol) of commercially available N719 dye (Solaronix Inc., Switzerland).¹⁶ The dye coated TiO₂ electrodes were infiltrated with commercially available redox electrolyte MPN-100 (Solaronix, Inc., Switzerland), containing 100 mM of tri-iodide in methoxypropionitrile and acetonitrile (volume ratio = 1:2), which added 0.1 M LiI to the mixed electrolyte. A conductive glass slide sputter-coated with 100 nm of Pt was used as the counter-electrode. Electrode spacing between the nanowire and counter-electrodes was ensured by use of a 25 μm thick spacer. The photocurrent density and photovoltage of the resulting devices were measured with active sample areas of $0.25\ \text{cm}^2$ through a metal mask, using AM 1.5G simulated sunlight produced by a 500 W Oriel Solar Simulator.

Results and Discussion

Figures 1(a) and 1(b) are field emission scanning electron microscope (Nova 600 nanoSEM, FEI), FESEM, cross-sectional image of an as-prepared nanowire array layer. The image shows a highly uniform and densely packed array of feather-like nanowires grown vertically from the substrate. The nanowires are separated by voids or open grain boundaries. The columnar growth typically seen in sputter deposited polycrystalline films have been described by Thornton using structure zone diagrams.^{17,18} Since the TiO₂ was deposited at a relatively low temperature, the mobility of the deposited atoms was low; hence the anatase nanowire layer appeared as an ‘under dense’ structure, denoted as a Zone 1 structure by Thornton.^{17,18} From the X-ray diffraction pattern (XRD; Scintag Inc., CA, USA; Bruker D8 Discover),

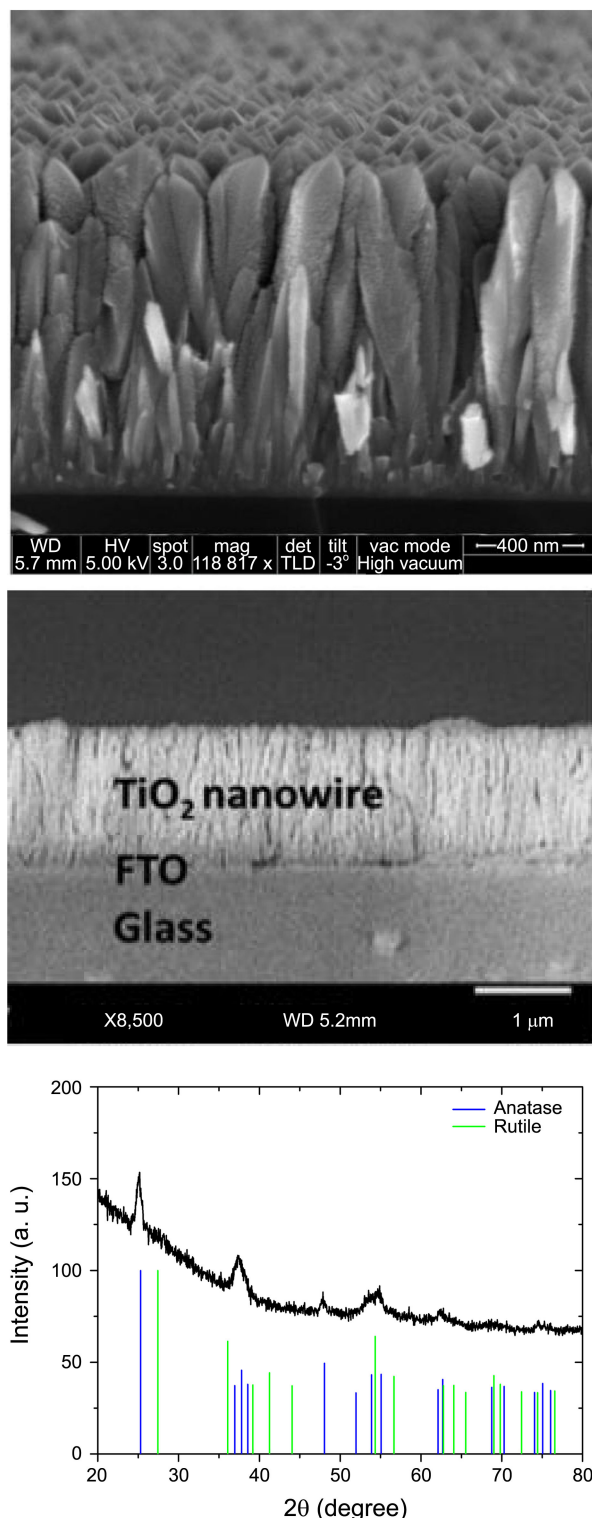


Figure 1. (a) FESEM images of vertically oriented feather-like TiO₂ nanowire arrays. (b) Cross-sectional image showing wires vertically oriented upon FTO-coated glass substrate. (c) X-ray diffraction pattern of nanowire array film deposited upon a Si (001) substrate.

Figure 1(c), the nanowires are classified as polycrystalline anatase with a grain size of approximately 20 nm estimated using the Scherrer formula. Figure 2(a) and Figure 2(b)

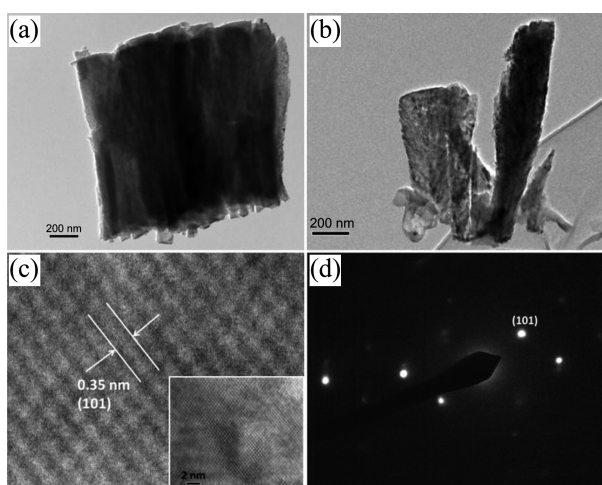


Figure 2. TEM images of nanowires. Shown are: (a) a bundle; (b) a single nanowire; (c) high-resolution image of anatase (101) lattice spacing (0.35 nm); and (d) selected-area electron diffraction pattern.

show, respectively, tunneling electron microscope (TEM; JEOL EM-2010, LaB6 Emitter) bright field images of a nanowire cluster and a single nanowire. A high resolution (HR) TEM image, Figure 2(c), shows a (101) crystal lattice plane of anatase phase with a d-spacing of 0.35 nm. The corresponding selected-area electron diffraction (SAED) pattern is shown in Figure 2(d); the clear diffraction spots reveal anatase phase in agreement with the XRD results. Each TiO_2 nanowire appears to be comprised of densely packed anatase grains. Figure 3 shows the UV-Vis absorbance (Perkin-Elmer Lambda 950) of an as-prepared nanowire array film 1 μm thick. There was neither discernable change to the crystallinity nor absorbance characteristics of the film with oxygen annealing (450 °C for up to 4 h); however, the conductivity of the FTO layer, as measured using a four-point probe (Model 280, Four Dimensions Inc.), decreased

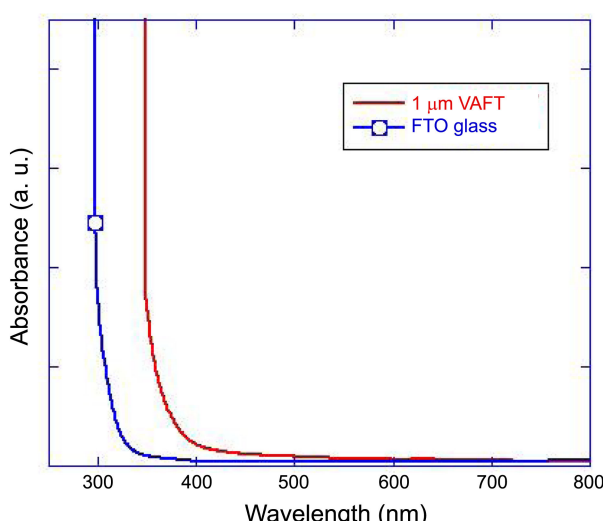


Figure 3. UV-Vis absorbance spectra of FTO coated glass, and same substrate upon which a 1 μm long nanowire array film has been grown.

approximately 8%.⁵

The nanowire array films were used as photoanodes in dye sensitized solar cells (DSSCs). Figure 4(a) shows the $J-V$ characteristics of DSSCs fabricated using nanowire array

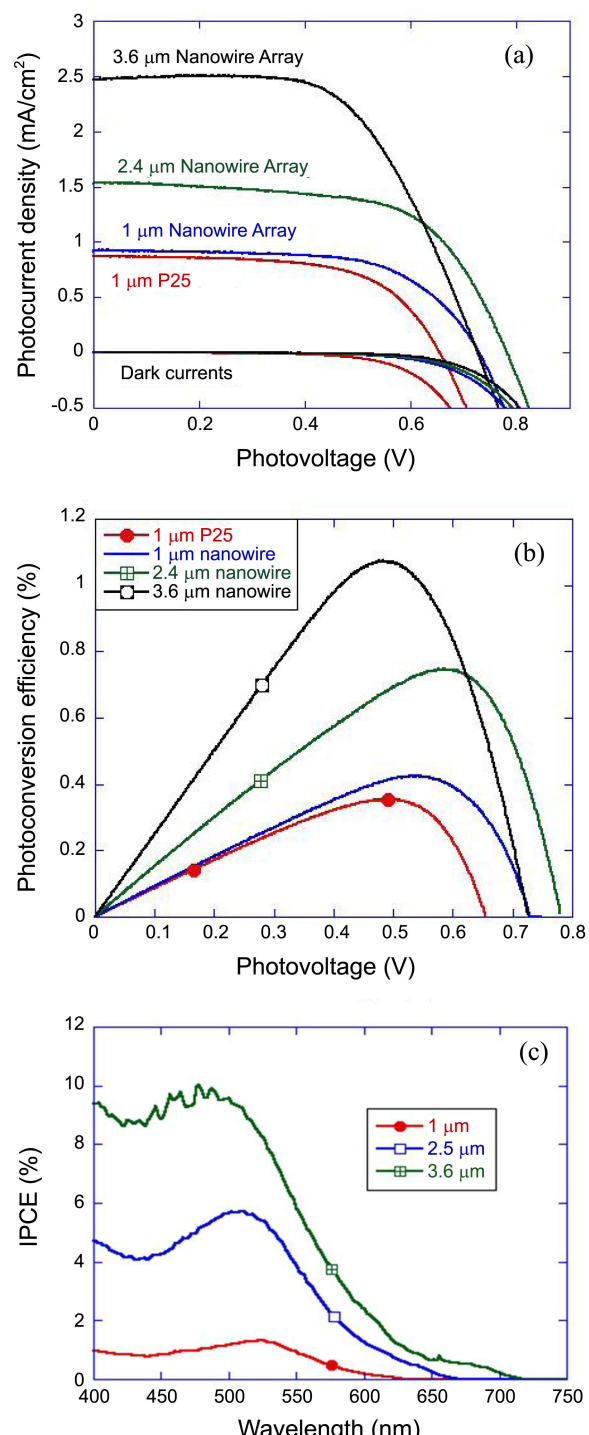


Figure 4. (a) Photocurrent density and dark current density of nanowire array films as a function of thickness, also show for comparison is the response of an otherwise identical DSSC that uses a 1 μm nanoparticle layer (Degussa P25) for the photoanode. (b) Corresponding photoconversion efficiency of the nanowire array films. (c) Corresponding incident photon to electron conversion efficiency (IPCE) of the nanowire array films.

Table 1. Summary of short circuit photocurrent density J_{sc} , open circuit voltage V_{oc} , fill factor and photoconversion efficiency η of different DSSCs

Sample	J_{sc} [mA/cm ²]	V_{oc} [V]	Fill Factor	η [%]
1 μm P25	0.87	0.65	0.62	0.35
1 μm nanowire	0.92	0.73	0.63	0.42
2.4 μm nanowire	1.53	0.78	0.63	0.75
3.6 μm nanowire	2.47	0.73	0.60	1.07

films of 1 μm, 2.4 μm and 3.6 μm length under AM 1.5G illumination with Table 1 summarizing device parameters. For comparison, the $J-V$ characteristics of a DSSC made using a 1 μm thick layer of Degussa P25 nanoparticles are also shown. AM1.5G power conversion efficiencies for the solar cells made using the 1 μm thick layer of VAFT have reached 0.42 %, compared to 0.35 % for solar cells made using the same thickness of P25 TiO₂. While we are still at the proof of principal stage in our work, the one-dimensional structure can offer the advantage of greater charge transport in a large surface area photoanode. This property may possibly enable an advance in DSSC performance. Figure 4(b) shows the photoconversion efficiency for the different devices, and Figure 4(c) the incident photon to collected electron conversion efficiencies (IPCE) which clearly shows that the longer nanowire array films significantly enhance the photoconversion of longer wavelength photons. DSSCs made with oxygen annealed nanowire array films showed a reduced photoconversion efficiency of approximately 5 to 8%, values in line with the measured decrease in the FTO layer conductivity.

Conclusion

Vertically aligned feather-like anatase phase TiO₂ nanowire arrays were successfully prepared on FTO coated glass substrates via pulsed DC magnetron sputtering at low temperature without degradation of the FTO conductivity. The nanowires consist of ≈ 20 nm grains. The synthesis technique is general, and can be readily extended to other metal oxide compositions. In our example, for the application of the anatase nanowire films in dye sensitized solar cells, we find a preliminary photoconversion efficiency of

1.07% for a nanowire photoanode 3.6 μm thick. The described synthetic method is cost-effective when compared to other synthetic schemes such as hydrothermal methods; but, of course, anatase nanowires on FTO coated glass have yet to be achieved by hydrothermal methods. Current efforts are focused on modifying deposition conditions to achieve single crystal nanowires of reduced feature size and greater length for increased surface area.

Acknowledgments. The authors thank Jinzhan Su and Keith Smerbeck for their helpful comments and suggestions.

References

1. O'Regan, B.; Grätzel, M. *Nature* **1991**, *353*, 737.
2. Bao, N.; Feng, X.; Grimes, C. A. *J. Nanotechnol.* **2012**, doi: 10.1155/2012/645931.
3. Mor, G. K.; Shankar, K.; Paulose, M.; Varghese, O. K.; Grimes, C. A. *Nano Lett.* **2006**, *6*, 215.
4. Zhu, K.; Neale, N. R.; Miedaner, A.; Frank, A. J. *Nano Lett.* **2007**, *7*, 69.
5. Varghese, O. K.; Paulose, M.; Grimes, C. A. *Nature Nanotechnol.* **2009**, *4*, 592.
6. Feng, X.; Shankar, K.; Varghese, O. K.; Paulose, M.; Latempa, T. J.; Grimes, C. A. *Nano Lett.* **2008**, *8*, 3781.
7. Liu, B.; Aydil, E. S. *J. American Chem. Soc.* **2009**, *131*, 3985.
8. Gong, D.; Grimes, C. A.; Varghese, O. K.; Hu, W. C.; Singh, R. S.; Chen, Z.; Dickey, E. C. *J. Mater. Res.* **2001**, *16*, 3331.
9. Paulose, M.; Shankar, K.; Yoriya, S.; Prakasam, H. E.; Varghese, O. K.; Mor, G. K.; Latempa, T. A.; Fitzgerald, A.; Grimes, C. A. *J. Phys. Chem. B* **2006**, *110*, 16179.
10. Prakasam, H. E.; Shankar, K.; Paulose, M.; Varghese, O. K.; Grimes, C. A. *J. Phys. Chem. C* **2007**, *111*, 7235.
11. Yoriya, S.; Mor, G. K.; Sharma, S.; Grimes, C. A. *J. Mater. Chem.* **2008**, *18*, 3332.
12. Yoriya, S.; Paulose, M.; Varghese, O. K.; Mor, G. K.; Grimes, C. A. *J. Phys. Chem. C* **2007**, *111*, 13770.
13. Shankar, K.; Mor, G. K.; Fitzgerald, A.; Grimes, C. A. *J. Phys. Chem. C* **2007**, *111*, 21.
14. Shankar, K.; Mor, G. K.; Prakasam, H. E.; Yoriya, S.; Paulose, M.; Varghese, O. K.; Grimes, C. A. *Nanotechnology* **2007**, *18*, Article No. 065707.
15. Varghese, O. K.; Gong, D. W.; Paulose, M.; Grimes, C. A.; Dickey, E. C. *J. Mater. Res.* **2003**, *18*, 156.
16. Snaith, H. J.; Schmidt-Mende, L. *Adv. Mater.* **2007**, *19*, 3187.
17. Thornton, J. A. *J. Vac. Sci. Tech.* **1974**, *11*, 666.
18. Thornton, J. A. *J. Vac. Sci. Tech.* **1975**, *12*, 830.